

## Neutron Transmutation Doping and Radiation Hardness for Solution-Grown Bulk and Nano-Structured ZnO

E. Flitsiyan<sup>a</sup>, C. Swartz<sup>a</sup>, R.E. Peale<sup>a</sup>, O. Lupan<sup>a,b</sup>, L. Chernyak<sup>a</sup>, L. Chow<sup>a</sup>, W.G. Vernetson<sup>c</sup>, Z. Dashevsky<sup>d</sup>

<sup>a</sup>Department of Physics, University of Central Florida, Orlando, FL 32816-2385, USA

<sup>b</sup>Department of Microelectronics and Semiconductor Devices, Technical University of Moldova, 2004 Chisinau, Republic of Moldova.

<sup>c</sup>Department of Nuclear and Radiological Engineering, University of Florida, Gainesville, Florida, 32611

<sup>d</sup>Department of Materials Engineering, Ben-Gurion University of the Negev, Beer-Sheva 84105, Israel

### ABSTRACT

It is shown that solution-grown ZnO nanostructures exhibit enhanced radiation hardness against neutron irradiation as compared to bulk material. The decrease of the cathodoluminescence intensity after irradiation at a neutron dose of  $6 \times 10^{16} \text{ cm}^{-2}$  in ZnO nanostructure is nearly identical to that induced by a dose of  $1.5 \times 10^{14} \text{ cm}^{-2}$  in bulk material. The damage introduced by irradiation is shown to change the nature of electronic transitions responsible for luminescence. The change of excitonic luminescence to the luminescence related to the tailing of the density of states caused by potential fluctuations occurs at an irradiation dose around  $6 \times 10^{16} \text{ cm}^{-2}$  and  $5 \times 10^{14} \text{ cm}^{-2}$  in nanostructured and bulk materials, respectively.

Hall measurements before and after annealing determined the effect of dose on resistance, mobility, and carrier concentration. Annealing decreased the sheet resistance, increased the mobility, and increased carrier concentration for all doses. While the concentration of carriers in the control sample increased 200-fold after annealing, the increase was ~1000-fold for the irradiated samples. Annealed irradiated samples showed a maximum carrier concentration increase of about 60x over the unirradiated sample. Interestingly, neutron irradiation increased the mobility even in the un-annealed samples.

### INTRODUCTION

ZnO is much more resistant to radiation damage than other common semiconductor materials, such as Si, GaAs, CdS and GaN<sup>1,2</sup>. Together with excellent optical and electrical properties, ZnO devices are therefore promising for space applications<sup>1</sup>. Difficulties in p-doping have been the main obstacle to realizing ZnO photonic devices. Better understanding of donor and acceptor behavior<sup>6,7</sup> is needed for development of ZnO *p-n* junctions. Knowledge of material property dependence on irradiation and thermal treatment is similarly important. The previous irradiation studies in ZnO were focused either on effects of electron or proton bombardment<sup>2,3</sup> or ion implantation.<sup>4,5</sup> Recently electrochemical nanostructuring of bulk GaN has been shown to enhance its radiation hardness against high energy heavy ion irradiation.<sup>6</sup> In this paper, effects of neutron irradiation with respect to transmutation doping and optical properties in bulk and nanostructured ZnO are studied.

### EXPERIMENT

ZnO nanorods were grown on quartz and Si substrates using facile and soft aqueous solution method without catalysts, templates and seeds. The synthesis route used here differs slightly from ordinary aqueous solution route. The substrates were cleaned in dilute HCl solution for 10 min and then rinsed in de-ionized (DI) water. Then the substrates were rinsed in ethanol/acetone (1:1) mixture, DI water, and dried in nitrogen, which gave uniformly wet-able

substrate surfaces. Starting materials were analytic-grade zinc sulfate and ammonia solutions (Fisher Scientific). Substrates were placed directly in the aqueous solution on a hot plate at 90 C for 15 min. The substrates were washed with DI water and the product dried in air at 150 C for 10 min. Phase purity and composition of the ZnO nanorods were examined by X-ray diffraction (XRD) using a Rigaku ‘D/B max’ X-ray diffractometer equipped with graphite monochromatized CuK $\alpha$  radiation ( $\lambda=1.54178 \text{ \AA}$ ) and operating conditions of 30 mA and 40 kV at a scanning rate of 0.02°/s in the 2 $\theta$  range of 10-90°.

Bulk ZnO hydrothermally-grown crystals were obtained from Air Force Research Lab, Hanscom AFB MA courtesy of Dr. David Bliss. Three bulk monocrystal ZnO samples were irradiated in the central vertical port of the University of Florida Training reactor (UFTR,  $5 \times 10^{13} \text{ n/cm}^2\text{-sec}$  thermal neutron flux) for 1, 10, and 20 hours. A fourth sample was reserved as a control. Neutron-irradiated and control ZnO samples were annealed at 600 °C for about one hour in flowing argon.

Six isotopes of Zn and three isotopes of O exist in nature:  $^{64}\text{Zn}$ (48.6, 0.74),  $^{65}\text{Zn}$ (27.9, 0.9),  $^{66}\text{Zn}$ (4.1, 6.9),  $^{67}\text{Zn}$ (18.8, 0.87),  $^{68}\text{Zn}$ (18.8, 0.87),  $^{70}\text{Zn}$ (0.6, 0.0091),  $^{16}\text{O}$ (99.78,  $1.9 \times 10^{-4}$ ),  $^{17}\text{O}$ (0.038,  $5.4 \times 10^{-4}$ ), and  $^{18}\text{O}$ (0.205,  $1.6 \times 10^{-4}$ ). The values in parantheses give the % natural abundance and thermal neutron capture cross section (barn). Some of the eight isotopes in ZnO are transmuted by interactions with thermal neutrons (energy ~25 meV). Fast neutron cross sections for the eight isotopes are insignificant. The relevant nuclear reactions are summarized in Table 1, where  $n$ ,  $\gamma$ ,  $e$ ,  $\nu$ , and  $\beta^-$  denote thermal neutron, gamma ray, electron, neutrino and beta ray, respectively. After the nuclear reactions  $^{64}\text{Zn}$ ,  $^{68}\text{Zn}$ ,  $^{70}\text{Zn}$  and  $^{18}\text{O}$  are transmuted to  $^{65}\text{Cu}$ ,  $^{69}\text{Ga}$ ,  $^{71}\text{Ga}$  and  $^{19}\text{F}$ , respectively. Isotope concentration  $C = C_i n \sigma f$ , where  $C_i$ ,  $n$ ,  $\sigma$ , and  $f$  are the constituent atom concentration, natural abundance, capture cross section, and thermal neutron flux, respectively. The calculated concentrations in  $\text{cm}^{-3}$  of generated isotopes for samples irradiated with neutron flux  $1.8 \times 10^{17} \text{ n/cm}^2$  are  $2.71 \times 10^{15}$ ,  $1.23 \times 10^{15}$ ,  $4.11 \times 10^{13}$ , and  $2.41 \times 10^9$  for  $^{65}\text{Cu}$ ,  $^{69}\text{Ga}$ ,  $^{71}\text{Ga}$ , and  $^{19}\text{F}$ , respectively.

**Table 1.** Nuclear reactions for Zn and O isotopes with thermal neutrons

Isotope	Nuclear Reaction	Half – life	Decay Energy
$^{64}\text{Zn}$	$^{64}\text{Zn} (n,\gamma) ^{65}\text{Zn} \quad ^{65}\text{Zn} \rightarrow ^{65}\text{Cu} + \gamma$	244.26days	1.352 MeV
$^{66}\text{Zn}$	$^{66}\text{Zn} (n,\gamma) ^{67}\text{Zn}$	Stable	-
$^{67}\text{Zn}$	$^{67}\text{Zn} (n,\gamma) ^{68}\text{Zn}$	Stable	-
$^{68}\text{Zn}$	$^{68}\text{Zn} (n,\gamma) ^{69}\text{Zn} \quad ^{69}\text{Zn} \rightarrow ^{69}\text{Ga} + \beta^-$	56.4 min	0.438 MeV
$^{70}\text{Zn}$	$^{70}\text{Zn} (n,\gamma) ^{71}\text{Zn} \quad ^{71}\text{Zn} \rightarrow ^{71}\text{Ga} + \beta^-$	2.45 min	2.813 MeV
$^{16}\text{O}$	$^{16}\text{O} (n,\gamma) ^{17}\text{O}$	Stable	-
$^{17}\text{O}$	$^{17}\text{O} (n,\gamma) ^{18}\text{O}$	Stable	-
$^{18}\text{O}$	$^{18}\text{O} (n,\gamma) ^{19}\text{O} \quad ^{19}\text{O} \rightarrow ^{19}\text{F} + \beta^-$	26.91 sec	4.821 MeV

Hall measurements before and after annealing determined the effect of dose on resistance, mobility, and carrier concentration. The experiment was conducted at room temperature using the Van der Pauw technique. Gold-platinum contacts were sputtered on each sample after which indium solder was used to attach copper wires from the contacts to the four poles of the Hall setup. Before annealing, contacts were removed by etching in nitric acid. Annealing was performed at 600°C for one hour in a constant flow of Ar.

Cathodoluminescence (CL) spectroscopy at 300 K used a Gatan MonoCL3 system integrated with a Philips XL 30 SEM. The CL was dispersed by a single grating (1200 lines/mm, blazed at

500 nm) and collected by a Hamamatsu photomultiplier tube. Excitation by the 20 keV electron beam corresponds to a 1.5  $\mu\text{m}$  penetration depth. The same SEM collected images of the CL-investigated areas.

## DISCUSSION

Gamma spectra of irradiated bulk ZnO reveal the characteristic 438.7 and 1117.4 keV lines corresponding to Zn-69 and Zn-65 radioactive isotopes, confirming the expected nuclear reactions (Table 1). Hall measurements of control and irradiated bulk samples showed n-type conduction. A comparison of electrical properties is presented in Figs.1 and 2. Annealing decreased the sheet resistance, increased the mobility, and increased carrier concentration for all doses. While the concentration of carriers in the control sample increased 200-fold after annealing, the increase was  $\sim 1000$ -fold for the irradiated samples. Annealed irradiated samples showed a maximum carrier concentration increase of about 60x over the unirradiated sample. Interestingly, neutron irradiation increased the mobility even in the un-annealed samples.

CL spectra are compared for bulk samples with zero and maximum dose in Fig. 3. All spectra feature a near-band-edge (NBE) emission at  $\sim 385$  nm and a broad band centered in the visible. Neutron irradiation evidently increases the intensity of the band-to-band transition by 30 % and shifts the visible band center from  $\sim 500$  to 580 nm. Integrated intensity is virtually unaffected by irradiation, but the emission is redistributed in favor of the NBE transition. NBE emission includes both conduction-band to neutral-acceptor transitions ( $e, A^0$ ) and shallow donor-acceptor pair (DAP) recombination<sup>3</sup>.

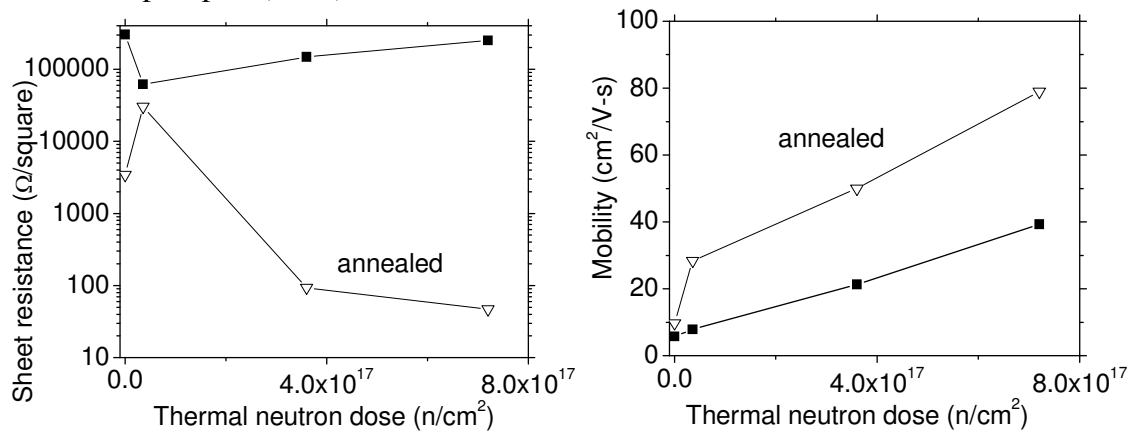


**Fig. 1.** (left) Comparison of sheet resistance in bulk ZnO samples as a function of dose with and without annealing. (right) Mobility determined from Hall measurements as a function of neutron dose and annealing.

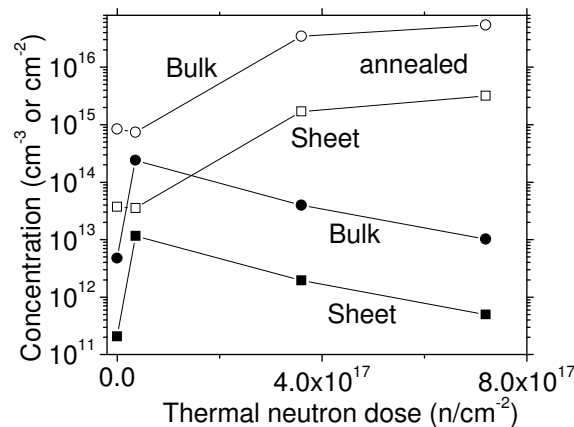


**Fig. 2.** Comparison of surface and bulk carrier concentrations.

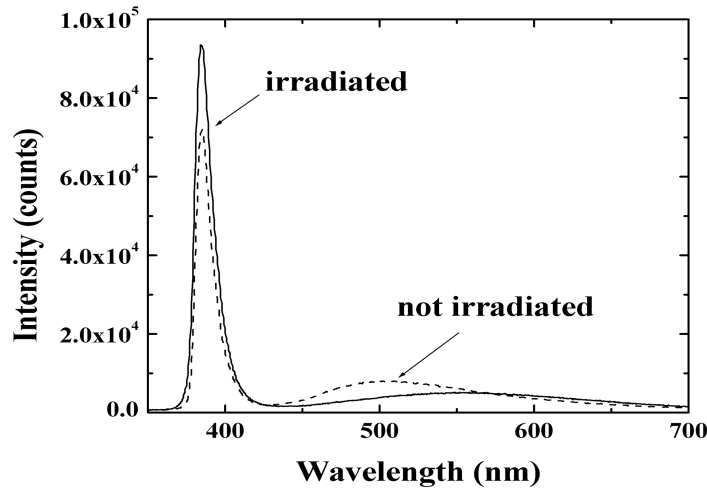


**Fig. 3.** Room temperature CL spectra of bulk sample 1 (solid line) and bulk sample 4 (dashed line).

Hence, the NBE intensity increase may indicate an increased concentration of shallow donors. The acceptor identity remains unclear, but Ga is a good candidate for the shallow donor since its level is located about 50 meV below the conduction band edge<sup>4</sup>.

Effects of annealing on the bulk sample subjected to the highest dose of irradiation are shown in Fig. 4. Annealing reduce the intensity of both peaks, indicating an increase of carrier lifetime. This is expected from improved crystallinity, as supported by the doubling of mobility (Fig. 1).

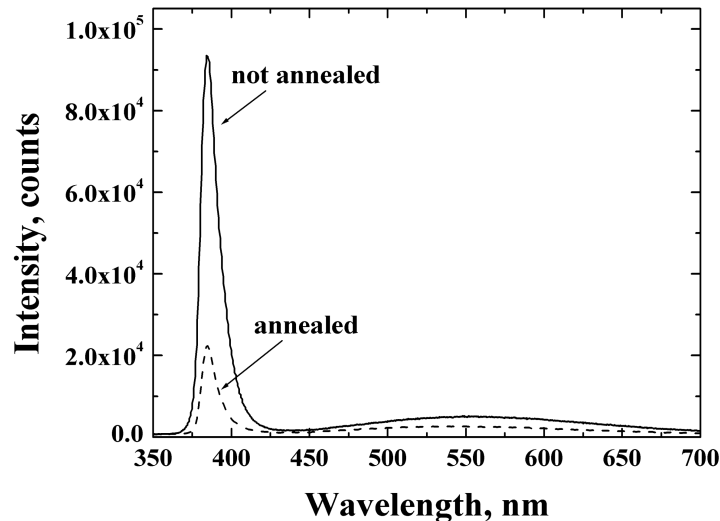


**Fig. 4.** Room temperature cathodoluminescence spectra of sample 4 before (solid line) and after (dashed line) annealing.

Nano-structured ZnO samples are considered next. The nanostructured and control bulk samples were irradiated by neutron doses  $1.5 \times 10^{14}$  n/cm<sup>2</sup>;  $6 \times 10^{14}$ ;  $1.5 \times 10^{15}$ ; and  $6 \times 10^{16}$  n/cm<sup>2</sup> in the vertical port of the University of Florida Training reactor.

Representative SEM micrographs are presented in Fig. 5. XRD peaks of 1D nanorods were indexed according to the hexagonal phase of ZnO (wurtzite structure,  $a = 0.3249$  nm,  $c = 0.5206$  nm) and the data are in agreement with the JCPDS 036-1451 card<sup>5</sup> for ZnO. No characteristic peaks of impurity phases such as Zn or S was observed and no diffraction peaks except those of

ZnO were found. The high intensity of the ZnO (002) peak indicated preferential growth along the c-axis in the [002] direction and good crystallinity of the samples.

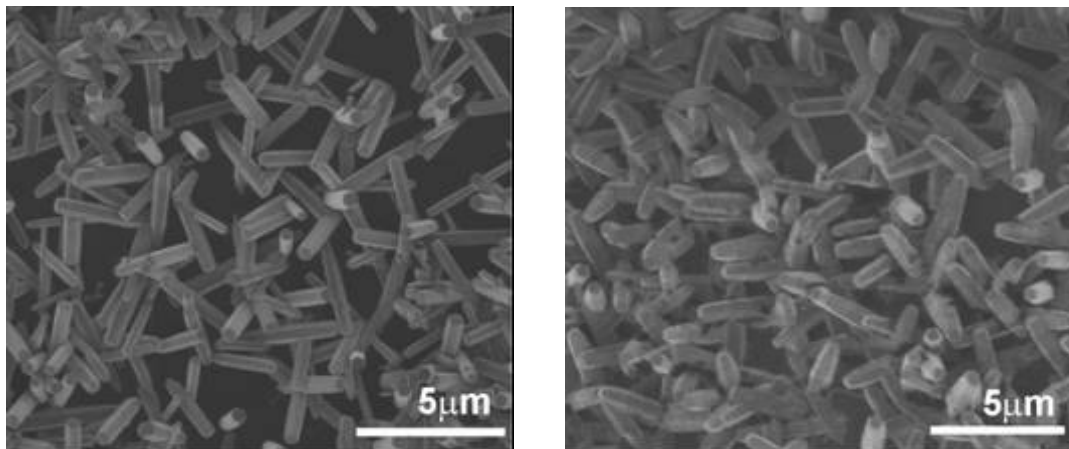


**Fig. 5.** SEM images of ZnO nanocrystals. Each image is of the region for which CL spectra were collected (Fig. 6). The left spectrum is of an as-grown sample, the right of an irradiated sample.

The CL spectra of ZnO nano-rod based sample (Fig. 6) reveal a strong and sharp UV emission at 385 nm, which corresponds to the near band edge emission of ZnO. The strong peak at 385 nm and weakness of the broad green emission band suggest that the nanorods possess high crystal quality with minimum oxygen vacancies. Neutron irradiation causes a blue shift of the NBE line and the appearance of a broad blue-green emission band for both nano- and mono-crystal samples.

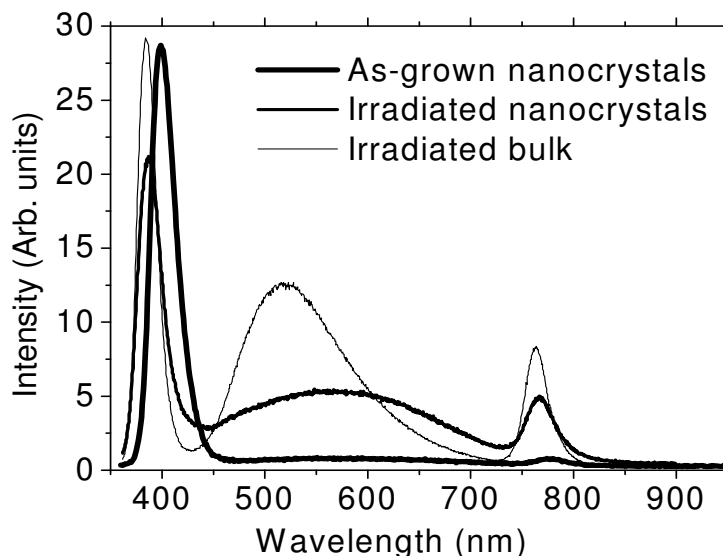


**Fig. 6.** Comparison of CL spectra of ZnO bulk and nano-rod samples for various irradiation conditions. The irradiated nano-rod sample received a neutron dose of  $6 \times 10^{16} \text{ n/cm}^2$ , while the bulk sample received  $1.5 \times 10^{14} \text{ n/cm}^2$ .

The low-energy emission can be the superposition of several contributions usually associated with oxygen vacancies, zinc interstitials<sup>6-8</sup>, and radiation defects and is therefore a measure of radiation hardness. The dose for the bulk sample was more than two orders of magnitude lower than for the nano-crystal sample, yet the radiation-defect band is considerably stronger, even

when the spectra are normalized to have the same NBE strength. This suggests that nano-crystalline ZnO is more radiation hard than bulk, in agreement with similar observations for GaN.

## CONCLUSIONS

Neutron irradiation damage changes the ZnO luminescence spectrum. Changes of excitonic emission that are likely related to the tailing of the density of states occurs at doses around  $6 \times 10^{16}$  n/cm<sup>2</sup> and  $1.5 \times 10^{14}$  n/cm<sup>2</sup> for nanorods and bulk, respectively. This is more than two orders of magnitude difference in dose. The superior radiation hardness for ZnO nanorods is likely due to the much higher specific surface area, which facilitates migration of the radiation defects toward the surface.

The high optical quality of the ZnO nanorods prepared by facile and soft aqueous solution method, combined with enhanced radiation hardness suggests that these structures are suitable for the development of optical devices able to operate in radiation harsh environments, particularly for space applications and microlasers. The nanolasers on ZnO nanorods are promising for many applications including optical computing, information storage and microanalysis<sup>9</sup>.

## ACKNOWLEDGMENTS

LC and ZD acknowledge partial support of the NATO grant CBP.MD.CLG 983122.

## REFERENCES

1. D. C. Look, D. C. Reynolds, J. W. Hemsky, R. L. Jones and J. R. Sizelove, "Production and annealing of electron irradiation damage in ZnO" *Appl. Phys. Lett.* **75**, 811 (1999).
2. F. Tuomisto, K. Saarinen, D. C. Look, and G. C. Farlow, "Introduction and recovery of point defects in electron-irradiated ZnO", *Phys. Rev. B* **72**, 085206 (2005).
3. K. Thonke, T. Gruber, N. Teofilov, R. Schonfelder, A. Waag and R. Sauer, "Donor-acceptor pair transitions in ZnO substrate material", *Physica B*, **308**, 945 (2001).
4. F. Reuss, C. Kirchner, T. Gruber, R. Kling, S. Maschek, W. Limmer, A. Waag and P. Ziemann, "Optical investigations on the annealing behavior of gallium- and nitrogen-implanted ZnO," *J. Appl. Phys.*, **95**, 3385 (2004).
5. Joint Committee on Powder Diffraction Standards, Powder Diffraction File No 36-1451.
6. W. L. Schaich, "Derivation of single-scattering formulas for x-ray-absorption and high-energy electron-loss spectroscopies", *Phys. Rev. B* **29**, 6513 - 6519 (1984)
7. R.T. Cox, D. Block, A. Herve, R. Picard, C. Santier, R. Helbig, Defect studies in electron-irradiated ZnO and GaN", *Solid State Commun.*, **25** (2), 77 (1978).
8. N.O. Korsunskaya, L.V. Borkovskaya, B.M. Bulakh, L.Yu. Khomenkova, V.I. Kushnirenko, I.V. Markevich, "The influence of defect drift in external electric field on green luminescence of ZnO single crystals", *J. Lumin.*, 102–103, 733 (2003).
9. M.H. Huang, S. Mao, H. Feick, H. Yan, Y. Wu, H. Kind, E. Weber, R. Russo, and P. Yang, "Room-Temperature Ultraviolet Nanowire Nanolasers", *Science* **292** 1897 (2001).